

Chemical and Physical Properties of Porous Silicon

Bo-Yeon Lee¹, Minwoo Hwang¹, Hyun Cho¹, Hee-Chol Kim¹ and Seunghyun Jang^{2†}

Abstract

The differences of properties for both single-layered and multi-layered porous silicon were investigated. Multistructured porous silicons such as DBR or rugate porous silicon exhibit strong reflection resonances providing the reflection of a specific wavelength in the optical reflectivity spectrum. DBR PSi displays a square varying porosity gradient in the direction perpendicular to the plane of the filter but a sinusoidally varying porosity gradient was obtained for rugate PSi.

Key words : Porous Silicon, Optical Property, Refractive Index, DBR, Rugate

1. Introduction

The development of new methods to build photonic structures in a device is of great interest, since conventional lithographic method is too complex to fabricate. An electrochemical etch is one of lithographic methods to fabricate a photonic structures into the materials. Since the discovery of porous silicon (PSi)^[1] multilayer-structured PSi has been intensively investigated for a variety of applications such as chemical^[2,3] and biological sensors^[4], medical diagnostics, optical band pass filters, micro chemical reactors, and micro fuel cells^[5-9]. Its importance is due to very high surface area as well as their unique photonic properties. Multilayered PSi is an attractive candidate for building photonic structure, because the porosity and average pore size can be tuned by adjusting the electrochemical preparation conditions that allow the construction of photonic crystals^[10,11]. Multilayer PSi such as distributed Bragg reflectors (DBR) PSi^[12] or rugate PSi^[13] exhibit unique optical properties providing a reflection band at specific wavelength in the optical reflectivity spectrum.

In this paper, the discriminations of properties of PSi for sing-layered, and multi-layered porous silicon (DBR PSi and rugate PSi) were described.

2. Experimental Section

2.1. Synthesis of Porous Silicon

The single layered PSi was prepared by an electrochemical etching of Si wafer (boron doped, polished on the <100> face, resistivity of 0.8 ~ 1.2 mΩ·cm, Siltronix, Inc.). The etching solution consisted of a 1:1 (v/v) mixture of absolute ethanol (ACS reagent, Aldrich Chemicals) and aqueous 48% hydrofluoric acid (ACS reagent, Aldrich Chemicals). Galvanostatic etching was carried out in a Teflon cell using an electrode configuration. The current density and etching time were 100 mA/cm² and 60 sec. The anodization current was supplied by Keithley 2420 high-precision constant current source controlled by a computer to allow the formation of PSi. To prevent the photogeneration of carriers, electrochemical etching was performed the anodization in the dark. All samples were then rinsed several times with ethanol and dried under argon atmosphere prior to use.

DBR PSi samples are prepared by electrochemical etch of heavily doped p⁺⁺-type silicon wafers (boron doped, polished on the (100) face, resistivity of 0.8 - 1.2 mΩ·cm, Siltronix, Inc.). The etching solution consisted of a 3:1 volume mixture of aqueous 48% hydrofluoric acid and absolute ethanol. DBR PSi samples are prepared by using a computer-generated periodic square wave current. DBR PSi samples exhibiting its reflectance at 570 nm have been prepared by using 5 mA/cm² for 60 s and 50 mA/cm² for 3 s with 20 repeats.

Rugate PSi samples were prepared by an electro-

¹Department of Chemistry, Chosun University, Gwangju, 501-759, South Korea

²Department of Chemistry, University of Wisconsin, Madison, 1101 University Ave., Madison, WI 53706 (USA)

*Corresponding author : shjang@chem.wisc.edu

(Received : July 2, 2011, Revised : August 16, 2011,

Accepted : August 31, 2011)

chemical etch of heavily doped p⁺⁺-type silicon wafers (boron doped, <100> oriented, resistivity of 0.8-1.2 mΩ·cm, Siltronix, Inc.). The etching solution consisted of a 3:1 volume mixture of aqueous 48% hydrofluoric acid and absolute ethanol. Rugate PSi samples were prepared by using a computer-generated sinusoidal current waveform with limits of 11 to 34 mA/cm², 100 repeats, and periods on the order of 8 sec depending on the desired wavelength of maximum reflectivity. The porous layers generated in the electrochemical etch were smooth enough to create high-quality 1D photonic crystals.

2.2. Instrumentation and Data Acquisition

The entire electrochemical process is carried out under constant current supplied by a computer controlled Keithley 2420 power sourcemeter. Optical reflectivity spectra are measured using a tungsten halogen lamp and an Ocean Optics S2000 CCD spectrometer fitted with a fiber optic input. The reflected light collection end of the fiber optic is positioned at the focal plane of the optical microscope. The morphology of PSi film and polymer replica were observed with cold field emission scanning electron microscope (FE-SEM, S-4700, Hitachi).

3. Result and Discussion

3.1. Monolayer- and Multilayer- Structured Porous Silicon

The multilayer structures based on PSi open the door for a variety of new applications. Some of the possible application of these structures are in the areas of interference filters^[14], waveguides^[15], photodiode^[16], and microcavities^[17]. For all these application, strict control over the reflectance and transmission properties of the PSi multilayer is required.

The advantage of a dielectric multilayer structure is the multiple interference a light beam undergoes when it is reflected at each interface. A qualitative representation of this is described in Figure 1, where interference from a single film is compared to a multilayer structure. The light beam is reflected at each interface between the two materials containing two different refractive indices. In a single layer (neglecting the multiple reflections of light between interface) the reflected light is composed of two reflectivity beams, one across the air-film interface and the other across the film-substrate interface (in Figure 1 A). In the case of the multilayer structure, the reflected light is a combination of all the reflectivity beams at each of the interface (in Figure 1 B, 5 reflected beams are observed). By simply choosing the thickness and refractive index of each of the layers, it is possible to control the constructive and destructive interference of the light across a multilayer structure, which dictates its reflectivity spectrum.

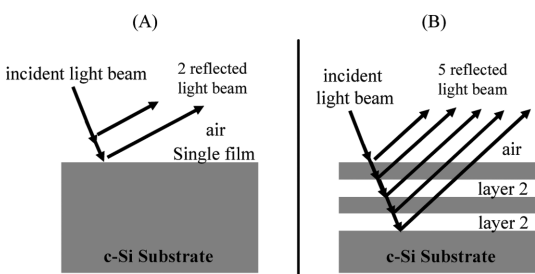


Fig. 1. Multiple interference of thin film structure. Representation of the reflection and transmission of light by a single (A) and a multilayer structure (B).

face (in Figure 1 A). In the case of the multilayer structure, the reflected light is a combination of all the reflectivity beams at each of the interface (in Figure 1 B, 5 reflected beams are observed). By simply choosing the thickness and refractive index of each of the layers, it is possible to control the constructive and destructive interference of the light across a multilayer structure, which dictates its reflectivity spectrum.

3.2. Properties of Multilayer Structures

PSi multilayers consist of alternating layers of different refractive index. PSi multilayer structures are easily manufactured using a periodic current density square waveform for distributed Bragg reflectors (DBR)^[18-22] and sinusoidal waveform for rugate^[23-26] during the electrochemical etching process as described in Figure 2. The difference in porosity profile, corresponding to a variation in current density, is attributed to a difference in refractive index.

The single layered PSi was prepared by an electrochemical etching of silicon wafer with an etching solution consisted of a mixture of absolute ethanol and hydrofluoric acid. PSi prepared by applying a current density exhibits high reflectivity in a general wide spectral region. The values of thickness and refractive index satisfy the following relationship:

$$m\lambda = 2nL \sin\theta. \quad (1)$$

Where λ is the wavelength of maximum constructive interference for spectral fringe of order m , n is the index of refraction of the porous layer and its contents, and L is the thickness of the porous layer. The optical thickness (OT) referred to as the quantity $2 nL$, was obtained

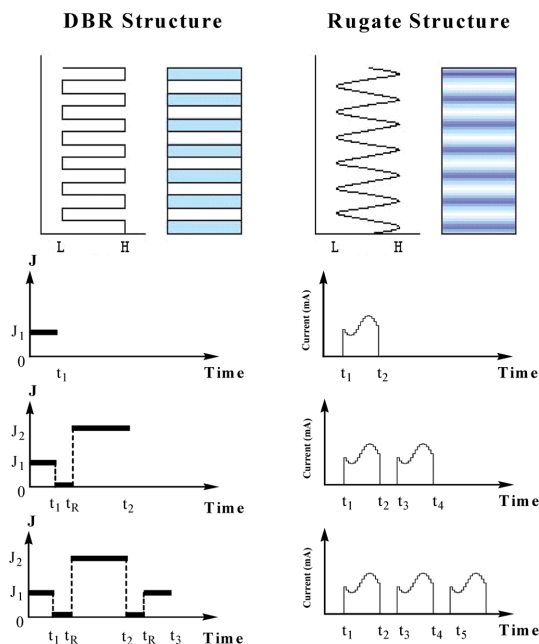


Fig. 2. Schematic pictures on the formation of PSi multilayer structures. By pulsing between two different current densities, two different porosity PSi layers can be formed (left) and step-functions used to approximate the sinusoidal variation of refractive index (right).

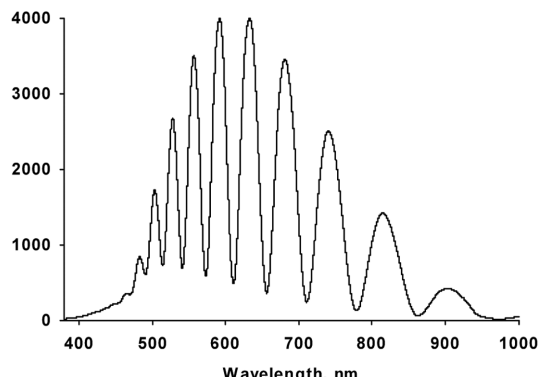


Fig. 3. Fabry-Perot fringes in the reflection spectra of PSi.

from Fourier transformation (FT) of the reflectivity spectrum. FT arising from a sharp resonance indicated the quantity $2 nL$. The PSi displayed Fabry-Perot fringes in the optical reflective spectra shown in Figure 3.

Multilayered porous silicon containing two distinct porosities has been successfully prepared by using a periodic galvanostatic electrochemical etch of crystal-

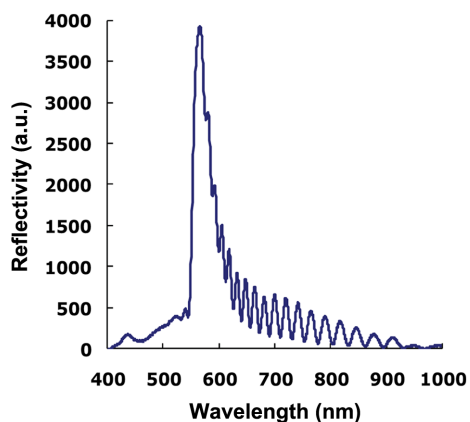


Fig. 4. Optical reflectivity spectrum of DBR PSi.

line silicon. The wavelength of a peak in the reflectivity spectrum is given by the following equation:

$$m\lambda_{\text{Bragg}} = 2 n_i d_i$$

where m is the spectral order of the optical fringe, λ the wavelength, n_i the refractive index of the film, and d_i its thickness. DBR PSi samples display a very sharp line at 570 nm with sidelobes around the reflectance peak in the optical reflectivity spectrum as shown in Figure 4. The spectral bands of DBR PSi samples have a full-width at half-maximum (FWHM) of about 20 nm.

The waveform used in the present work involves a sine component, which is represented by

$$Y = A \cdot \sin(kt) + B$$

where Y represents a temporal sine wave of amplitude A , frequency k , time t , and an applied current density B . The position of reflection band depends on the frequency. Rugate porous silicon has been successfully prepared using a periodic galvanostatic electrochemical etch of crystalline silicon by applying a sine wave current. The applied current density is modulated with a pseudo sine wave to generate a periodically varying porosity gradient. Rugate PSi samples display a very sharp reflection line at 510 nm without sidelobes around the reflectance peak in the optical reflectivity spectrum as shown in Figure 5. The spectral band of rugate PSi sample has a full-width at halfmaximum (FWHM) of about 17 nm.

Multistructured PSi, DBR or rugate, exhibit unique

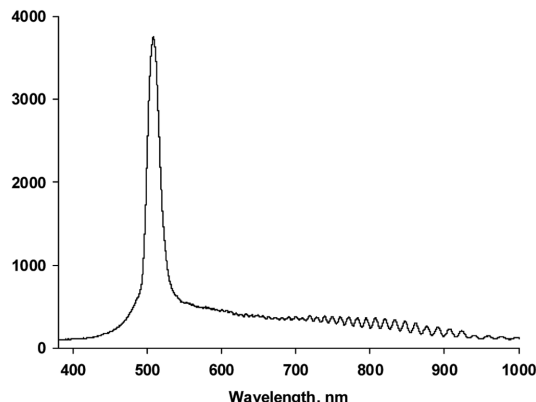


Fig. 5. Optical reflectivity spectrum of Rugate PSi.

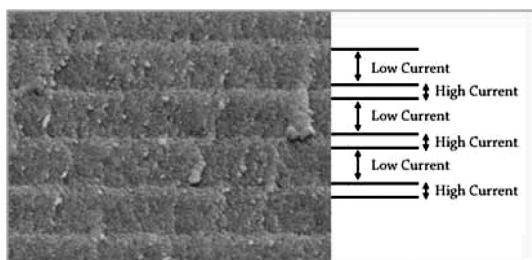


Fig. 6. Cross-sectional image of DBR PSi.

optical properties providing the reflection of a specific wavelength in the optical reflectivity spectrum. This reflective wavelength can be controlled by tuning of many etching parameters and can appear anywhere in the visible range.

Figure 6 shows a cross-sectional SEM image of a PSi multilayer where the different layers present alternating porosity (refractive index) layers. The two parameters that govern the optical properties of the multilayers are the thickness and refractive index of the alternating layers, so control over these properties is critical. Other properties like interface roughness and depth homogeneity also affect the quality of the multilayer structures. SEM images shown in Figure 6 were obtained using a cold field emission scanning electron microscope (FE-SEM, S-4800, Hitachi). The cross-sectional image of DBR PSi shown illustrates that the multilayer DBR PSi has a depth of few microns. A repeating etch process results in two distinct refractive indices and displays a square varying porosity gradient in the direction perpendicular to the plane of the filter for DBR PSi.

The cross-sectional FE-SEM images of rugate PSi

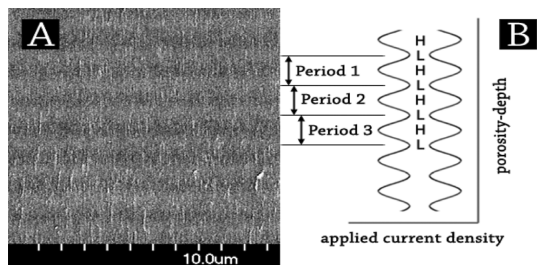


Fig. 7. Cross-sectional image of rugate PSi.

shown in Figure 7 illustrate that the thickness of rugate PSi is about few microns. FE-SEM image of rugate PSi displays a sinusoidally varying porosity gradient in the direction perpendicular to the plane of the filter. FE-SEM image of rugate PSi indicates that the prepared rugate PSi has cylindrical mesopores with the average pore size of few nanometers.

4. Conclusion

The properties of single-layered and multi-layered porous silicon, such as optical properties and morphology were investigated. Multistructured PSi, DBR or rugate, exhibit unique optical properties providing the reflection of a specific wavelength in the optical reflectivity spectrum. A repeating etch process results in two distinct refractive indices and displays a square varying porosity gradient in the direction perpendicular to the plane of the filter for DBR PSi. A sinusoidally varying porosity gradient in the direction perpendicular to the plane of the filter was obtained for rugate PSi

References

- [1] Uhrlir, A, "Electrolytic shaping of germanium and silicon", Bell System Tech, Vol. 35, p. 333, 1956.
- [2] M. W. Hwang and S. D. Cho, "Detection of Organic Vapors Using Change of Fabry-Perot Fringe Pattern of Surface Functionalized Porous Silicon", J. Am. Chem. Soc., Vol 3, No. 3, p. 168, 2010.
- [3] D. H. Jung, "Biosensor Based on Distributed Bragg Reflector Photonic Crystals for the Detection of Protein A", Journal of the Chosun Natural Science, Vol. 3, No. 1, p. 33, 2010.
- [4] H. J. Kwon, "Fabrication and Characterization of Silole and Biotin-functionalized Rugate Porous Silicon", Journal of the Chosun Natural Science, Vol.

- 3, No. 1, p. 24, 2010.
- [5] S. H. Jang, "Study on Thickness of Porous Silicon Layer According to the Various Anodization Times", *Journal of the Chosun Natural Science*, Vol. 3, No. 4, p. 206, 2010.
- [6] B. Y. Lee, M. W. Hwang, H. Cho, H. C. Kim, and S. D. Cho, "Preparation and Optical Characterization of Photonic Crystal Smart Dust Encoded with Reflection Resonance", *Journal of the Chosun Natural Science*, Vol. 3, No. 2, p. 84, 2010.
- [7] Khan, M. A., Haque, M. S., Naseem, H. A., Brown, W. D., and Malshe, "Microwave plasma chemical vapor deposition of diamond films with low residual stress on large area porous silicon substrates", *A. P. Thin Solid Films*, Vol. 332, p. 93, 1998.
- [8] H. Sohn, "Detection of Volatile Alcohol Vapors Using Silicon Quantum Dots Based on Porous Silicon", *Journal of the Chosun Natural Science*, Vol. 3, No. 2, p. 117, 2010.
- [9] Zhai, L., A Nolte, J. R., Cohen, E. and Rubner, M. F., "pH-Gated Porosity Transitions of Polyelectrolyte Multilayers in Confined Geometries and Their Application as Tunable Bragg Reflectors", *Macromolecules*, Vol. 37, p. 6113, 2004.
- [10] J. M. Han, "Photoluminescence of Porous Silicon According to Various Etching Times and Various Applied Current Densities", *Journal of the Chosun Natural Science*, Vol. 3, No. 3, p. 148, 2010.
- [11] S. H. Jang, "Investigation of Relationship between Etch Current and Morphology and Porosity of Porous Silicon", Vol. 3, No. 4, p. 210, 2010.
- [12] T. E. Choi, J. S. Yang, S. Y. Um, S. H. Jin, B. M. Cho, S. D. Cho, and H. Sohn, "Preparation and Optical Characterization of DBR/Host Dual Porous Silicon Containing DBR and Host Structures", *Journal of the Chosun Natural Science*, Vol. 3, No. 2, p. 84, 2010.
- [13] Y. H. Kwon, "Characteristic Analysis of Band Width Based on Rugate Porous Silicon Containing Photonic Nanocrystal", *Journal of the Chosun Natural Science*, Vol. 2, No. 1, p. 41, 2010.
- [14] M. G. Berger, C. Dieker, M. Thonisen, L. Vescan, H. Luth, and H. Munder, "Porosity superlattices: a new class of Si heterostructures", *J. Phys. D*, Vol. 27, p. 1333, 1994.
- [15] A. Loni, L. T. Canham, M. G. Berger, R. Arens-
- Fisher, H. Munder, H. Luth, H. F. Arrand, and T. M. Benson, "Porous silicon multilayer optical waveguides", *Thin Solid Films*, Vol. 276, p. 143, 1996.
- [16] M. Hruger, M. G. Berger, M. Marso, W. Reetz, T. Eickhoff, R. Loo, L. Vescan, M. Thonissen, H. H. Luth, R. Arens-Fischer, S. Hilbrich, and W. Theiss, *Jpn. J. Appl. Phys.* 36, L24 (1997).
- [17] C. Delerue, G. Allan, and M. Lannoo, "Theoretical aspects of the luminescence of porous silicon", *Phys. Rev. B*, Vol. 48, p. 11024, 1993.
- [18] C. Mazzoleni and L. Pavesi, "Application to optical components of dielectric porous silicon multilayers", *Appl. Phys. Lett.*, Vol. 67, p. 2983, 1995.
- [19] M. G. Berger, R. Arens-Fischer, M. Thonisson, M. Kruger, S. Billat, H. Luth, S. Hilbrich, W. Theiss, and P. Grosse, "Dielectric filters made of PS: advanced performance by oxidation and new layer structures", *Thin Solid Films*, Vol. 297, p. 237, 1997.
- [20] M. Cazzanelli, C. Vinegoni, and L. Pavesi, "Temperature dependence of the photoluminescence of all-porous-silicon optical microcavities", *J. Appl. Phys.*, Vol. 85, p. 1760, 1999.
- [21] V. Lehmann, R. Stengl, H. Reisinger, R. Detemple, and W. Theiss, "Optical shortpass filters based on macroporous silicon", *Appl. Phys. Lett.*, Vol. 78, p. 589, 2001.
- [22] V. Agarwal and J. A. del Rio, "Tailoring the photonic band gap of a porous silicon dielectric mirror", *Appl. Phys. lett.*, Vol. 82, p. 1512, 2003.
- [23] B.G. Bovard, "Rugate filter theory: an overview", *Appl. Opt.* Vol. 32, p. 5427, 1993.
- [24] A. J. Nolte, M. F. Rubner, and R. E. Cohen, "Creating Effective Refractive Index Gradients within Polyelectrolyte Multilayer Films: Molecularly Assembled Rugate Filters", *Langmuir*, Vol. 20, p. 3304, 2004.
- [25] J. R. Dorvee, A. M. Derfus, S. N. Bhatia, and M. J. Sailor, "Manipulation of liquid droplets using amphiphilic, magnetic one-dimensional photonic crystal chaperones", *Nat. Mater.* Vol. 3, p. 896, 2004.
- [26] S. Ilyas, T. B?cking, K. Kilian, P. J. Reece, J. Gooding, K. Gaus, and M. Gal, "Porous silicon based narrow line-width rugate filters", *Opt. Mater.*, Vol. 29, p. 619, 2007.